# Xestospongins: Potent Membrane Permeable Blockers of the Inositol 1,4,5-Trisphosphate Receptor

**ARTICLE** *in* NEURON · OCTOBER 1997

Impact Factor: 15.05 · DOI: 10.1016/S0896-6273(00)80384-0 · Source: PubMed



**7 AUTHORS**, INCLUDING:

Tadeusz F Molinski
University of California, San Diego
**222** PUBLICATIONS **5,981** CITATIONS

SEE PROFILE

Isaac Pessah
University of California, Davis
**283** PUBLICATIONS **9,887** CITATIONS

SEE PROFILE

Neuron, Vol. 19, 723–733, September, 1997, Copyright ©1997 by Cell Press

# Xestospongins: Potent Membrane Permeable Blockers of the Inositol 1,4,5-Trisphosphate Receptor

**Juliette Gafni,* Julia A. Munsch,† Tien H. Lam,* Michelle C. Catlin,‡ Lucio G. Costa,‡ Tadeusz F. Molinski,† and Isaac N. Pessah*§**
*Department of Molecular Biosciences
School of Veterinary Medicine
and Graduate Program in Neurosciences
†Department of Chemistry
University of California
Davis, California 95616
‡Department of Environmental Health
University of Washington
Seattle, Washington 98195

## Summary

**Xestospongins (Xe's) A, C, D, araguspongine B, and demethylxestospongin B, a group of macrocyclic bis-1-oxaquinolizidines isolated from the Australian sponge, Xestospongia species, are shown to be potent blockers of $IP_3$-mediated $Ca^{2+}$ release from endoplasmic reticulum vesicles of rabbit cerebellum. XeC blocks $IP_3$-induced $Ca^{2+}$ release ($IC_{50}$ = 358 nM) without interacting with the $IP_3$-binding site, suggesting a mechanism that is independent of the $IP_3$ effector site. Analysis of Pheochormocytoma cells and primary astrocytes loaded with $Ca^{2+}$-sensitive dye reveals that XeC selectively blocks bradykinin- and carbamylcholine-induced $Ca^{2+}$ efflux from endoplasmic reticulum stores. Xe's represent a new class of potent, membrane permeable $IP_3$ receptor blockers exhibiting a high selectivity over ryanodine receptors. Xe's are a valuable tool for investigating the structure and function of $IP_3$ receptors and $Ca^{2+}$ signaling in neuronal and nonneuronal cells.**

## Introduction

The phosphoinositide signaling cascade plays a prominent role in neuronal signaling. High levels of the inositol 1,4,5-trisphosphate receptor ($IP_3R$) are expressed in the cerebellum, hippocampus, cerebral cortex, corpus striatum, and olfactory tubercule (Verma et al., 1990). Stimulation of the $IP_3R$ results in $Ca^{2+}$ mobilization from intracellular stores, which in turn activates many cellular processes, including neuromodulation, synaptic plasticity, and sensory perception (Berridge, 1993). Stimulation of G protein–linked or tyrosine kinase–linked cell surface receptors leads not only to production of $IP_3$ and subsequent $Ca^{2+}$ release from endoplasmic reticulum (ER) stores, but also to coordinated activation of intracellular enzymes such as protein kinase C, phosphatidylinositol 3-OH kinase, and GTPase-activating protein.

In order to define the importance of the $IP_3R$ in neuronal processes, selective, membrane permeable blockers of the $IP_3R$ are needed. Whereas selective antagonists of the large variety of cell surface receptors are known (Brann et al., 1993; Arrang, 1994; Pin and Duvoisin, 1995), chemical probes that selectively target the $IP_3R$ are currently limited to heparin and $IP_3R$ antibodies. The usefulness of heparin is limited due to its low affinity, lack of selectivity, membrane impermeability, and targeting of the $IP_3$-binding site (Ghosh et al., 1988; Kobayashi et al., 1988). Evidence that heparin inhibits the synthesis of $IP_3$ (Berridge, 1993), and stimulates ryanodine-sensitive $Ca^{2+}$ release (Bezprozvanny et al., 1993) have further complicated interpretation of results aimed at understanding the role of the $IP_3R$ in cellular processes. Three $IP_3R$ antibodies have been shown to block $IP_3$-induced $Ca^{2+}$ release. The 18A10 monoclonal antibody binds to the proposed $Ca^{2+}$ channel region in the carboxy-terminus of the receptor protein (amino acid residues 2736–2747), inhibiting $IP_3$-induced $Ca^{2+}$ release in cerebellar microsomes (Nakade et al., 1991). Two other $IP_3R$ inhibitory serums have been developed, one targeting the 420 residues within the "coupling" domain (amino acid residues 1379–1798) and the other binding to the 95 residues near the C-terminus (amino acid residues 2604–2698) (Sullivan et al., 1995). Both of these antibodies block $IP_3$-stimulated $Ca^{2+}$ release and nuclear envelope assembly in Xenopus egg extracts (Sullivan et al., 1995). The main disadvantage of $IP_3R$ inhibitory antibodies is that they are membrane impermeable and thus require specialized techniques (i.e., injection, patching onto cells) and/or disruption of cellular integrity (i.e., patching or permeabilization of cells) to access the $IP_3R$.

Since a large number of biologically active compounds isolated from marine organisms have been shown to interact with cellular receptors (Crews et al., 1994), we screened 120 species of marine sponges for $IP_3R$ inhibitory activity. We found one sponge, Xestospongia species, to contain five potent blockers of $IP_3$-mediated $Ca^{2+}$ release ($IC_{50}$s ranging from 358 nM to 5.9 μM). Structure elucidation revealed the active principles to be the bis-1-oxaquinolizidines xestospongin A (XeA), xestospongin C (XeC), xestospongin D (XeD), araguspongine B (ArB), and demethylxestospongin B (DMXeB). Interestingly, XeA, XeC, and XeD were isolated by Nakagawa et al. (1984) and recognized for their vasodilative activity.

In the present study, we demonstrate that XeA, XeC, XeD, ArB, and DMXeB are potent blockers of $IP_3$-induced $Ca^{2+}$ release from isolated cerebellar microsomes, and display a high selectivity over the skeletal isoform of the ryanodine receptor (type 1; $Ry_1R$). The most potent of these blockers, XeC, is a membrane permeable blocker of $IP_3$-mediated $Ca^{2+}$ release in intact cells. A simple model is presented that relates structural aspects of the xestospongin/araguspongine family of 1-oxaquinolizidine alkaloids to their potency at the $IP_3R$. XeC provides an ideal pharmacological tool for investigating the structure of the $IP_3R$, as well as $IP_3$-mediated $Ca^{2+}$ signaling in neuronal and nonneuronal cells.

§To whom correspondence should be addressed.

A

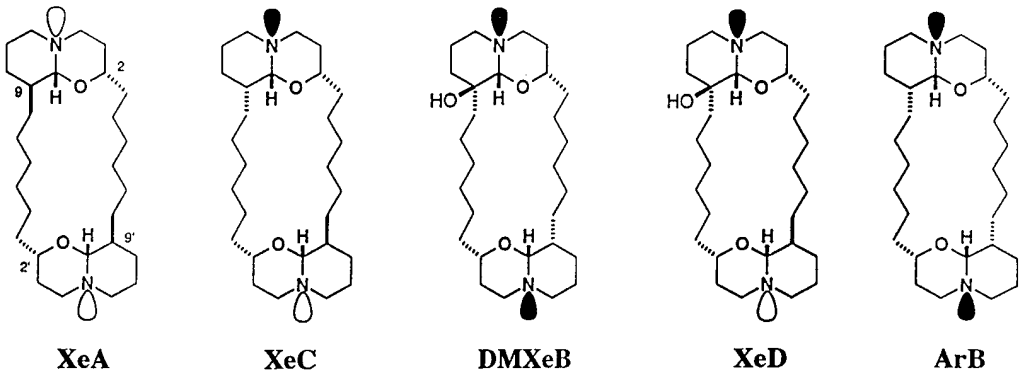


B

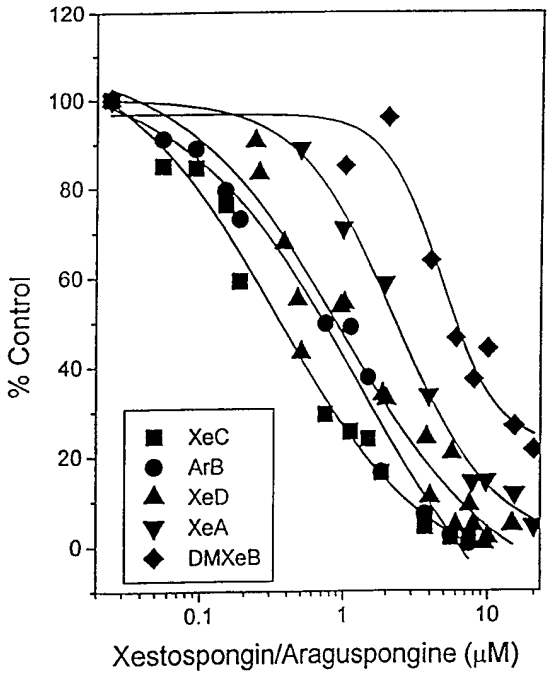


Figure 1. Bis-1-Oxaquinolizidines Isolated from Xestospongia Species Are Potent $IP_3R$ Blockers

(A) Xe and araguspongine structures were extracted and purified from the Australian sponge, Xestospongia species, and tested for their ability to block $IP_3$-induced $Ca^{2+}$ release from cerebellar microsomes.

(B) Inhibition of $IP_3$-induced $Ca^{2+}$ release from actively loaded cerebellar microsomes was used to determine the potency of the Xe/araguspongine congeners tested. The $IC_{50}$ values for the five congeners ranged from 358 nM to 5.9 μM (see text for details). Data from each compound are fit to a single site model, and curves for XeC, ArB, XeD, and XeA represent the average of two experiments performed on two different cerebellar microsomal preparations. The DMXeB curve is an average of three experiments. The mean rate (±SD) of $Ca^{2+}$ release for control was 7.0 ± 2.0 nmol $Ca^{2+}$ $s^{-1}$ $mg^{-1}$ with 5 μM $IP_3$.

## Results and Discussion

### Subcellular Calcium Transport and Binding Studies

$IP_3$-induced $Ca^{2+}$ transport across actively loaded rabbit cerebellar microsomes was initially used to screen 120 crude MeOH extracts from 120 species of sponges for $IP_3R$ inhibitory activity. Five potent $IP_3R$ inhibitors were then isolated from Xestospongia species, the only sponge containing potent $IP_3R$ inhibitors, using the mechanism-based assay (Figure 1A). The specificity of the assay for detecting $IP_3$-mediated $Ca^{2+}$ changes was

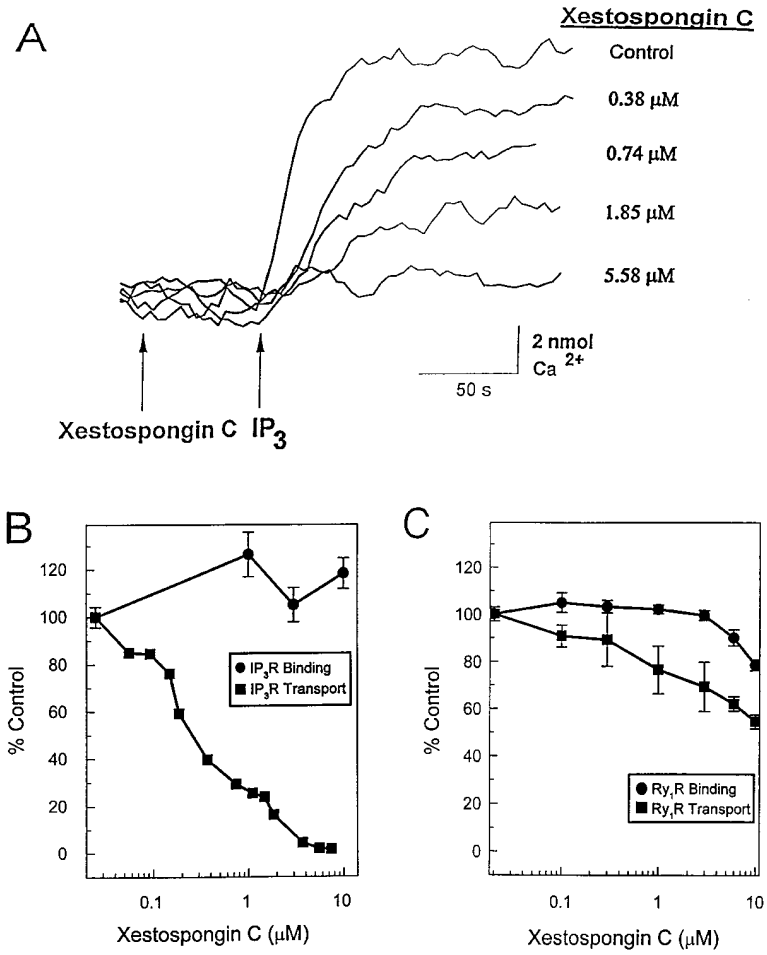


Figure 2. XeC Blocks $IP_3$-Induced $Ca^{2+}$ Release by a Mechanism Independent of the $IP_3$-Binding Site

(A) Raw traces showing XeC blocks $IP_3$ (5 μM)-induced $Ca^{2+}$ release from cerebellar microsomes in a dose-dependent manner.

(B) The dose–response curve for XeC is fit to a multisite model to illustrate the multiphasic nature of inhibition, whereas XeC (1–10 μM) does not affect the ability of $[^3H]IP_3$ (1 nM) to bind to cerebellar microsomes (200 μg protein).

(C) XeC is >30-fold less potent toward blocking [$^3$H]ryanodine binding and caffeine-induced $Ca^{2+}$ release in skeletal SR. XeC (0.1–10 μM) blocked [$^3$H]ryanodine (1 nM) binding and caffeine (20 mM)-induced $Ca^{2+}$ release to a much lesser extent in $Ca^{2+}$-loaded skeletal vesicles (50 μg protein) enriched in $Ry_1R$. The control rate (±SD) of caffeine-induced $Ca^{2+}$ release averaged 28.4 ± 6.0 nmol $Ca^{2+}$ $s^{-1}$ $mg^{-1}$.

initially tested. $IP_3$-induced $Ca^{2+}$ release was stereoselective, since $Ca^{2+}$ efflux from cerebellar microsomes occurred only following addition of the D- (not L-) $IP_3$ enantiomer. Heparin (≥20 μM), a known $IP_3R$ inhibitor, also blocked $IP_3$-induced $Ca^{2+}$ release from cerebellar microsomes, further verifying that $IP_3$-mediated $Ca^{2+}$ release was being selectively measured. In addition, saturating concentrations (7.5–20 μM) of XeA, XeC, XeD, ArB, or DMXeB did not alter the absorbance of antipyrylazo III or the $Ca^{2+}$ calibration of the dye, verifying that Xe's did not interfere with the ability of antipyrylazo III to detect changes in extramicrosomal $Ca^{2+}$.

Inhibition curves for XeA, XeC, XeD, ArB, and DMXeB were obtained by measuring $Ca^{2+}$ transport in cerebellar microsomes. For each compound, duplicate experiments using two different cerebellar microsomal preparations were performed to construct the inhibition curves shown in Figure 1B. All Xe's blocked $IP_3$-mediated $Ca^{2+}$ release in a dose-dependent manner. XeC, which contains one *cis*-fused and one *trans*-fused oxaquinolizidine, proved to be the most potent $IP_3R$ inhibitor with an $IC_{50}$ of 358 nM. The *cis*/*trans* combination exhibited superior inhibition of $IP_3$-induced $Ca^{2+}$ release, when compared to the *trans*/*trans* system in XeA, which has a nearly 10-fold larger $IC_{50}$ of 2535 nM. It is not clear whether the *cis*/*trans* system is truly a more potent inhibitor than the *cis*/*cis* system in ArB, which has an $IC_{50}$ of 648 nM, since ArB was not purified to homogeneity (~75 mol % purity). The addition of a hydroxyl group to C9 of XeC (XeD) diminished the potency of the *cis*/*trans* system and elevated the $IC_{50}$ to 844 nM. Substituting the *cis*-fused oxaquinolizidine of XeD for a *trans*-fused oxaquinolizidine (DMXeB) reduced inhibition of $IP_3$-induced $Ca^{2+}$ release by nearly an order of magnitude, raising the $IC_{50}$ to 5865 nM.

While the more potent Xe's (XeC, ArB, XeD) tended to produce a multiphasic inhibition of $IP_3$-induced $Ca^{2+}$ release from cerebellar microsomes, equivalent concentrations of XeC had no effect on the specific binding of $[^3H]IP_3$ to the same membrane vesicles (Figures 2A and 2B). For example, 10 μM XeC did not produce a decrease in specific $[^3H]IP_3$ binding, even though 7.5 μM of XeC completely blocked $IP_3$-mediated $Ca^{2+}$ release, indicating a noncompetitive mechanism with respect to the $IP_3$-binding site. The apparent multiphasic nature of Xe inhibition curves (Figure 2B [XeC]) could be explained by the existence of multiple $IP_3R$ isoforms in the microsomal preparations from whole cerebella, which may have different affinities for Xe's. At least three isoforms of the $IP_3R$ have been identified and cloned (Furuichi et al., 1989; Mignery et al., 1990; Südhof et al., 1991; Ross et al., 1992; Maranto, 1994; Yamada et al., 1994; Harnick et al., 1995), and there is evidence that the cerebellum contains more than one of these isoforms (Nakanishi

et al., 1991; Ross et al., 1992). [$^3$H]Ryanodine binding studies and caffeine-mediated $Ca^{2+}$ transport assays using rabbit skeletal sarcoplasmic reticulum (SR) preparations showed that XeC also dose dependently interacts with the $Ry_1R$ (Figure 2C). XeC (10 $\mu$M) decreased [$^3$H]ryanodine binding by 22% and caffeine-induced $Ca^{2+}$ release by 46%, indicating that XeC can interact with the $Ry_1R$, but in a significantly less potent manner. The $IC_{50}$ for blocking caffeine-induced $Ca^{2+}$ release with XeC was (greater than 30-fold its $IC_{50}$ for blocking $IP_3$-mediated $Ca^{2+}$ release from the $IP_3R$. Differences in Xe potency toward $IP_3R$ and $Ry_1R$ blockade may also reflect variations in amino acid sequences, especially around the putative pore-forming region (Furuichi et al., 1989; Mignery et al., 1989, 1990; Takeshima et al., 1989).

The mechanism by which Xe's block $IP_3$-induced $Ca^{2+}$ release could be the result of either: (1) block of the $Ca^{2+}$ channel pore, or (2) an allosteric mechanism that uncouples $IP_3$ binding from $Ca^{2+}$ release. Although the present study does not discriminate between the two possible mechanisms, the chemical structure of Xe's, a lipophilic elongated core with two partially charged N groups at either end, provide an ideal lipophilic/hydrophilic moiety to fit into the $IP_3R$ channel pore. Tinker and Williams (1995) used a series of monovalent and divalent trimethylammonium derivatives, which bear structural resemblance to Xe's, to define the length of the pore of $Ry_2R$ (cardiac isoform) reconstituted in bilayer lipid membranes. Based on the relative potency for pore blockade, they concluded a pore distance of 10.4 Å. Interestingly, their estimate is consistent with the molecular distance between the partially charged tertiary nitrogens of XeC (11.6 Å). Despite the very similar molecular structures of Xe's, some useful empirical correlations can be drawn regarding how structure relates to potency toward inhibition of $IP_3$-induced $Ca^{2+}$ release. Two important considerations in this respect are net charge and molecular dimensions. The free bases of Xe are relatively lipophilic molecules and readily soluble in chloroform or methanol. The bridgehead nitrogen of the oxaquinolizidine ring system is moderately basic having a pKa of $\sim$11 for the protonated form. At pH 7.0, the average charge on the bis-oxaquinolizidine molecule is between $+1.5$ and $+2.0$, distributed between the two tertiary nitrogens. The molecular structures of XeA, XeC, and ArB differ only with respect to stereochemistry at the oxaquinolizidine ring junction and configurations at C2,2′ and C9,9′, the points of attachment of the methylene side chains. Therefore, XeA, XeC, and ArB are diastereomers. XeA has the more stable *trans* ring junction in both oxaquinolizidine rings and diequatorial substituents at C2 and C9, which are disposed *trans* to each other. By contrast, XeC differs from XeA in possessing the energetically less favorable *cis* ring junction stereochemistry in one of the oxaquinolizidine rings with diequatorial substituents at C2 and C9 that are *cis* to each other. Clearly the *cis*, *trans* orientation of XeC is favored for the $IP_3R$ since it exhibits a 7-fold higher potency compared to XeA. The 2-fold rotationally ($C_{2v}$) symmetric ArB (Kitagawa et al., 1989; Hoye et al., 1994, 1995) has *cis* ring fusions and *cis* C2,9 substituents (axial at C9 to the piperidine rings) in both heterobicycles. Unfortunately, interpretations about how the structure of ArB relates to $IP_3R$ channel activity are thus far precluded since ArB could not be purified to homogeneity, and the structures of impurities remain to be elucidated. XeD and DMXeB are 9-hydroxy derivatives of XeC and ArB, respectively. Although addition of an axial OH group at C9 in XeD does not increase the molecular cross section (see below), the added polarity and/or introduction of an H-bond donor decreases potency $\sim$2.4-fold. The 16-fold decrease in potency seen with DMXeB is likely to be mainly due to the *cis* ring fusions and *cis* C2,9 substituents in both heterobicycles, with a smaller contribution from the OH group at C9. In this respect, the potent activity seen with the ArB fraction may be attributed to a yet to be identified Xe. XeC has been shown by X-ray crystallography to have a long narrow rod-like shape, and this feature is preserved in the calculated MM2 structure. The calculated van der Waals profile was defined by a rectangle of width of 8.22 Å, height of 5.78 Å, and molecular cross section of 47.6 Å$^2$. The molecular cross section (Å$^2$) is defined here as the area of a rectangular whose sides are the minimum van der Waals height and width of the narrowest projection or profile of the MM2 minimized structure. In this respect, the OH moiety of XeD does not contribute to the molecular cross section (47.6 Å$^2$) and only produces a small (2.4-fold) decrease in receptor potency. A major structural consequence of stereochemical differences between the alkaloids related to XeC is a significant change in molecular cross section. Inverting the configurations at both the bridgehead nitrogen and C9 of the flexible *cis*, *trans* C2,9 diequatorial (bent) configuration of XeC to the flattened, more rigid *trans*, *trans* C2,9 diequatorial configuration of XeA widens the molecule in order to accommodate bowing of the methylene chains between the two oxaquinolizidine moieties and reduces potency more significantly (7-fold). The van der Waals profile changes accordingly to a width of 9.38 Å, a height of 5.34 Å, and an overall larger molecular cross section (49.8 Å$^2$). Thus, the molecular dimensions of Xe's appear to be more important in defining potency for $IP_3R$ channel blockade than the presence of an OH at C9, although the presence of the latter disrupts some yet undefined aspect of the interaction with $IP_3$ receptors. Despite the importance of the cross-sectional area in determining the structure–activity relationship, there are clearly other factors contributing to this relationship. For example, the $>$16-fold decrease in potency of DMXeB (relative to XeC) could be attributed to the fact that the two *cis*-fused oxaquinolizide rings of DMXeB are more conformationally flexible than the mixed junctions of XeC. Further experiments are needed to determine the XeC binding site and refine the current model.

### Cytosolic Calcium Measurements in Intact PC12 Cells and Astrocytes

Pheochormocytoma (PC12) cells have been shown to respond to bradykinin with increased production of $IP_3$ and transient elevations in cytosolic $Ca^{2+}$ (Fasolato et al., 1991; Grohovaz et al., 1992). Xe's were shown to be effective $IP_3R$ blockers in fura 2–loaded PC12 cells by measuring cytosolic changes in $Ca^{2+}$ following bradykinin addition. Measurements performed in $Ca^{2+}$ replete

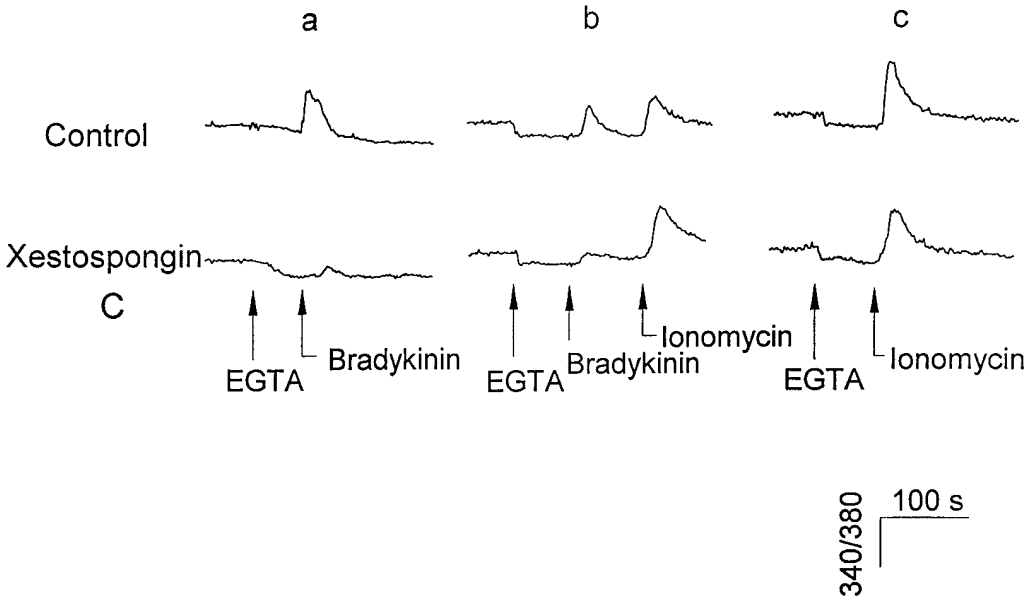


Figure 3. XeC Blocks Bradykinin Responsiveness of PC12 Cells in $Ca^{2+}$-Depleted Media without Altering the Levels of $Ca^{2+}$ Remaining in the Stores

Fluorometric measurements in PC12 cells using fura-2 AM (5 μg/ml) and $Ca^{2+}$-depleted media (120 nM and 40 nM $Ca^{2+}$) show that XeC (20 μM) blocks the peak response to bradykinin (300 nM)-induced $Ca^{2+}$ release. In the presence of 40 nM intracellular $Ca^{2+}$, addition of ionomycin (5 μM) in place of bradykinin shows that $Ca^{2+}$ stores are equal at the time of bradykinin addition. Each trace is a typical response from triplicate readings. Traces are reported as arbitrary fluorescence units (340 nm/380 nm). The vertical bar represents 1.0 arbitrary fluorescence ratio units. Column a, $[Ca^{2+}]_e$ = 120 nM; column b and c, $[Ca^{2+}]_e$ = 40 nM.

medium (2 mM) revealed that a 10 min application of 20 μM XeC reduced the peak of the bradykinin (300 nM)-induced $Ca^{2+}$ transient by 66 ± 5% of control (±SD; n = 4 determinations). Studies using $Ca^{2+}$-depleted media (120 and 40 nM free $Ca^{2+}$) indicated that addition of 20 μM XeC for 10 min blocked bradykinin-induced $Ca^{2+}$ release in PC12 cells to a similar extent as PC12 cells bathed in $Ca^{2+}$ replete buffer (Figure 3). Addition of ionomycin (5 μM) in place of bradykinin revealed that treatment of PC12 cells with 20 μM XeC for 10 min did not significantly affect the level of $Ca^{2+}$ in the stores (Figure 3). Fluorometric measurements of PC12 cells without bovine serum albumin (BSA) and/or a lengthened incubation time of 30 min revealed that XeC more effectively targeted the $IP_3R$ in the absence of BSA and with extended incubation times (data not shown). XeC appears to be maximally effective at blocking bradykinin-induced $Ca^{2+}$ release at bath concentrations of XeC as low as 10 μM, whereas 5 μM XeC results in a bradykinin-induced $Ca^{2+}$ mobilization, which is comparable to control levels (Figure 4). Reintroduction of $Ca^{2+}$ to the extracellular medium ($[Ca^{2+}]_e$ = 2 mM) following bradykinin stimulation showed that capacitative $Ca^{2+}$ influx is reduced proportionally in the presence of 10 and 20 μM XeC (Figure 4). Interestingly, subsequent thapsigargin (500 nM) addition revealed that the $Ca^{2+}$ leak from the ER is significantly reduced in the presence of 10 or 20 μM XeC (Figure 4).

Experiments aimed at determining whether XeC could discriminate between $IP_3$- and ryanodine-sensitive stores were conducted using ratiofluorescence imaging of fura 2–loaded PC12 cells, a neuronal cell model, which has both ryanodine- and $IP_3$-sensitive stores (Zacchetti et al., 1991). Addition of caffeine (30 mM) to the extracellular medium resulted in a transient rise in intracellular $Ca^{2+}$ (Figure 5A). Pretreatment of cells with 20 μM XeC for 10 min prior to addition of caffeine did not significantly alter the magnitude of the response to the ryanodine receptor (RyR) ligand (Figure 5B; Table 1). PC12 cells also vigorously responded to 50 μM ryanodine with a sustained rise in cytosolic $Ca^{2+}$ (Figure 5C). Subsequent addition of bradykinin (100 nM) induced an additional but transient rise in cytosolic $Ca^{2+}$. Addition of XeC (20 μM) 10 min prior to ryanodine did not quantitatively alter the peak response from the ryanodine-sensitive store (peak response [±SD] = 0.16 ± 0.03 and 0.18 ± 0.02 ratio units for control and XeC treatment, respectively; Figure 5D; Table 1). Subsequent addition of bradykinin produced a negligible response from the $IP_3$-sensitive store. In PC12 cells, ryanodine (50 μM) induced ER $Ca^{2+}$ release from the same store affected by caffeine, as demonstrated by the sequential addition of these compounds (Figure 5E). Addition of caffeine followed by ryanodine also demonstrated a common ryanodine/caffeine-sensitive store (data not shown). Taken together, the results in PC12 cells demonstrate that XeC can discriminate between ryanodine- and $IP_3$-sensitive $Ca^{2+}$ efflux pathways in intact PC12 cells. PC12 cells acutely treated with Xe's displayed no overt signs of cytotoxicity. Application of 20 μM XeC for 30 min did not induce trypan blue dye leakage into the cytosol of PC12 cells (zero cells stained/two dishes [35 $mm^2$]), indicating a viable cell population.

Xe's were also shown to block muscarinic-mediated

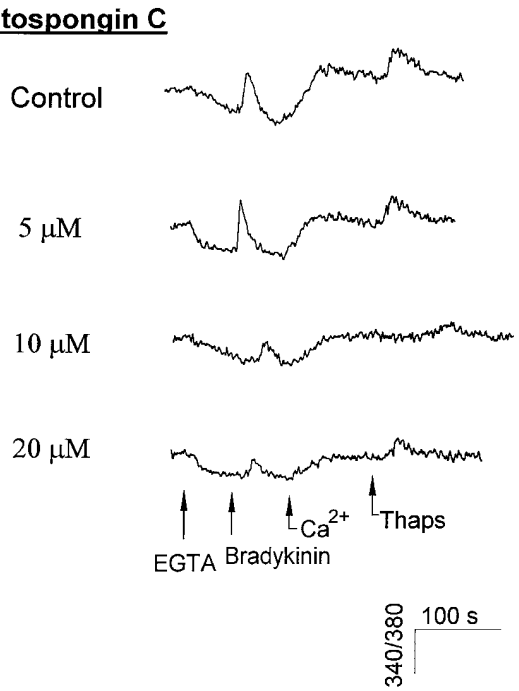


Figure 4. XeC Dose Dependently Blocks Bradykinin-Induced $Ca^{2+}$ Release in PC12 Cells

Fluorometric measurements using fura-2 AM (5 μg/ml) and $Ca^{2+}$-depleted media (120 nM) show that 20 and 10 μM XeC maximally block the peak response to bradykinin (300 nM)-induced $Ca^{2+}$ release, while 5 μM XeC has no significant effect. Following the reintroduction of $Ca^{2+}$ ($[Ca^{2+}]_e$ = 2 mM), thapsigargin (500 nM) was added to quantitate the ER $Ca^{2+}$ leak. Each trace is a typical response from duplicate experiments. The vertical bar represents 0.5 arbitrary fluorescence ratio units.

$IP_3$-induced $Ca^{2+}$ release in primary astrocytes, following addition of carbachol. Using confocal fluorescent microscopy, XeC (20 μM) was shown to block $IP_3$-induced $Ca^{2+}$ release and oscillations in primary astrocytes (Figures 6A and 6B). In addition, XeA was shown to block $IP_3$-induced $Ca^{2+}$ release in a concentration-dependent manner, with 20 μM XeA completely blocking $Ca^{2+}$ release and oscillations in most cells (Figures 6C–6F). Treatment of astrocyte cultures with 20 μM XeC for 30 min did not cause leakage of lactate dehydrogenase (LDH) into the media (untreated = 3.34 U/l; treated = 2.55 U/l).

Data provided from PC12 cells and primary astrocytes demonstrate that Xe's block phosphoinositide signaling regardless of the agonist used (bradykinin and carbamylcholine, respectively), revealing the general usefulness of these compounds. Further characterization of XeC's effects in PC12 cells provides insight into the $Ca^{2+}$ dynamics of intact cells. Application of ionomycin in place of bradykinin shows that blockade of the $IP_3R$ with XeC does not alter $Ca^{2+}$ store levels in PC12 cells (Figure 3). Reintroduction of $Ca^{2+}$ following bradykinin addition shows that blockade of $IP_3$-mediated $Ca^{2+}$ release with XeC causes a decrease in $Ca^{2+}$ entry that is proportional to the reduction in $Ca^{2+}$ release from intracellular stores (Figure 4), which supports current theory on capacitative $Ca^{2+}$ entry. A potentially important new finding with XeC is the substantial reduction in the ER $Ca^{2+}$ leak unmasked by thapsigargin, a smooth ER $Ca^{2+}$ pump inhibitor (Figure 4). The XeC-mediated reduction in the ER $Ca^{2+}$ leak may be attributed to blockade of the conformationally distinct leak states of the Ry and/or $IP_3$ receptor. In this respect, ryanodine-sensitive and insensitive ("leak") $Ca^{2+}$ efflux pathways in skeletal SR (Pessah et al., 1997) and ER $Ca^{2+}$ "leakage" via the $IP_3R$ in brain (Cameron et al., 1995) have been demonstrated. Considering the structural and functional similarity of Ry and $IP_3$ receptors, the present results support a dual role ($Ca^{2+}$ channel and $Ca^{2+}$ leak) for this class of ER/SR proteins (Cameron et al., 1995; Marks, 1996; Pessah et al., 1997). Xe's not only represent an optimal probe to study $IP_3$-mediated signaling processes and $Ca^{2+}$ dynamics in intact cells, but provide a unique pharmacological tool to further investigate the structure and functional properties of isolated $IP_3$-gated channels.

In conclusion, the present paper demonstrates that Xe's represent a new class of blockers of $IP_3$-induced $Ca^{2+}$ release from isolated ER membrane vesicles having nanomolar to micromolar affinity. The membrane permeant properties of Xe's also make them very useful tools for studying $IP_3$-mediated signaling in preparations of intact cells. Their ability to discriminate between ryanodine- and $IP_3$-sensitive stores in intact cells provides a distinct advantage to currently available inhibitors. Although the lipophilic elongated hydrocarbon core undoubtedly contributes to the cell permeant properties of Xe's, it may also promote appreciable partitioning of Xe's into cellular membrane lipids. The latter could account for the need to use 10–20 μM in the bath to attain sufficient concentrations of Xe at the ER surface. However, the physicochemical properties of XeC, which requires higher concentrations in cell culture, do not limit the selectivity of XeC for $IP_3R$ over RyR in PC12 cells (Figure 5), nor do they induce acute cytotoxicity. The actual concentrations of XeC reaching the ER surface are probably significantly lower than those applied to the extracellular medium.

Xe's can be used to further our understanding of the large variety of $IP_3$-mediated signaling pathways currently identified in neuronal and nonneuronal cells. In this respect, previous research has already shown that Xe's disrupt $IP_3R$-mediated cellular processes. Three Xe's (XeA, XeC, and XeD), originally isolated by Nakagawa et al. (1984), were identified as vasodilative compounds since they increased blood flow in the coronary, vertebral, and femoral arteries of anesthetized dogs (Nakagawa et al., 1984; Endo et al., 1986). Kitagawa et al. (1989) subsequently reported the vasodilative properties of XeA when the compound was infused into an isolated mesenteric artery preparation from the Sprague-Dawley rat, corroborating the findings of Nakagawa et al. XeD and DMXeB have also been shown to display growth-inhibitory activity in tumor cell lines and/or Micrococcus luteus (Quirion et al., 1992; Pettit et al., 1996). XeD and DMXeB were found to inhibit murine leukemia (L1210, $ED_{50}$ = 0.2, 0.8 μg/ml, respectively) and human epidermoid carcinoma (KB, $ED_{50}$ = 2.0, 2.5 μg/ml, respectively) cell growth activity (Quirion et al., 1992). XeD has also shown growth-inhibitory activity

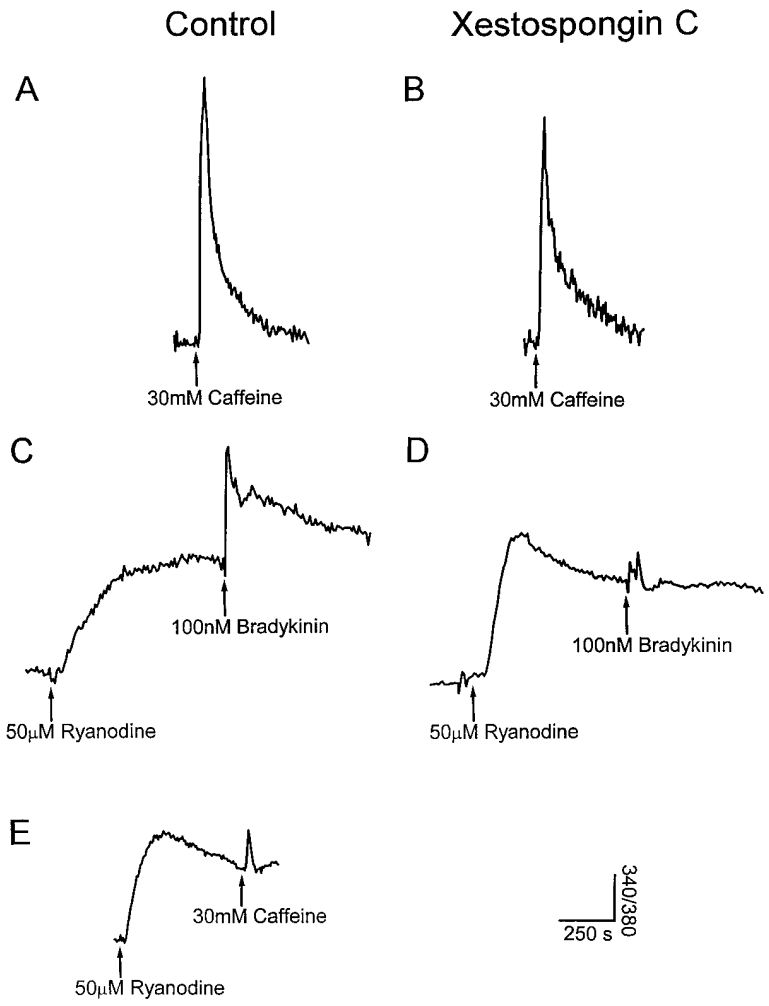


Figure 5. XeC Discriminates between Ryanodine- and $IP_3$-Sensitive Stores in PC12 Cells

Fluorometric measurements using fura-2 AM (5 μg/ml) and $Ca^{2+}$ (2 mM)-replete media show that PC12 cells possess ryanodine- and $IP_3$-sensitive $Ca^{2+}$ stores. Traces under control were treated with 4 μl MeOH 10 min prior to caffeine (A) or ryanodine ([C] and [E]) addition. Traces under XeC were treated with 20 μM XeC (in 4 μl MeOH) 10 min prior to addition of caffeine (B) or ryanodine (D). The vertical bar represents 0.05 arbitrary fluorescence ratio units. Table 1 summarizes the peak responses to RyR ligands in the presence and absence of XeC.

in a variety of leukemia (CCRF-CEM, HL-60TB, K-562, MOLT-4, and SR) and breast tumor (MCF7, HS 578T, MDA-MB-435, and MDA-N) cell lines (averaged $GI_{50}$ = 3.62 and 4.53 μM, respectively) and in the bacterium Micrococcus luteus (12.5–25 μg/6 mm disk) (Pettit et al., 1996). The vasodilative and growth-inhibitory activity of Xe's are consistent with their newly recognized $IP_3R$ channel-blocking activity, since vasoconstriction and cell division require $IP_3$-mediated $Ca^{2+}$ release (Berridge, 1993; Briner et al., 1993; Dauphin et al., 1994; Bretschneider et al., 1995a, 1995b; Sullivan et al., 1995).

Table 1. XeC Inhibits $IP_3$-Mediated $Ca^{2+}$ Release without Significantly Influencing Ryanodine-Sensitive Stores in PC12 Cells

| Treatment | Peak Response[a] (340/380 ± SD) |
|---|---|
| Bradykinin | |
| Control (n = 10) | 0.12 ± 0.03 |
| 20 μM XeC (n = 15) | 0.04 ± 0.01 |
| Caffeine | |
| Control (n = 18) | 0.40 ± 0.16 |
| 20 μM XeC (n = 20) | 0.47 ± 0.28 |
| Ryanodine | |
| Control (n = 10) | 0.16 ± 0.03 |
| 20 μM XeC (n = 15) | 0.18 ± 0.02 |

[a]Peak response is the average maximal change in arbitrary fluorescence units (340 nm–380 nm) to addition of 300 nM bradykinin following or 50 μM ryanodine treatment, 30 mM caffeine. The data represent the mean ± SD of the number of determinations indicated in parentheses in column 1. Repesentative traces are shown in Figure 5.

## Experimental Procedures

### Materials

D-*myo*-inositol 1,4,5-trisphosphate and L-*myo*-inositol 1,4,5-trisphosphate were obtained from LC Laboratories (Woburn, MA). Sodium heparin (MW 6000) was purchased from Sigma (St. Louis). [$^3$H]D-*myo*-inositol 1,4,5-trisphosphate (specific activity, 21 Ci/mmol) and [$^3$H]ryanodine (specific activity, 81.5 Ci/mmol; purity, >99%) were obtained from New England Nuclear (Wilmington, DE). High-purity ryanodine (>99%; used in radioligand receptor binding assays) and ryanodine mixture (1:3 ryanodine–dehydroryanodine; used in whole cell experiments) were purchased from Calbiochem (San Diego, CA). Bradykinin was obtained from Peptides International (Louisville, KY) and carbachol from Sigma (St. Louis). All other chemicals used were of the highest grade possible.

### Collection of Xe's

Two samples (A and B) of the marine sponge Xestospongia species (Phylum Porifera) were collected by hand using SCUBA at two sites

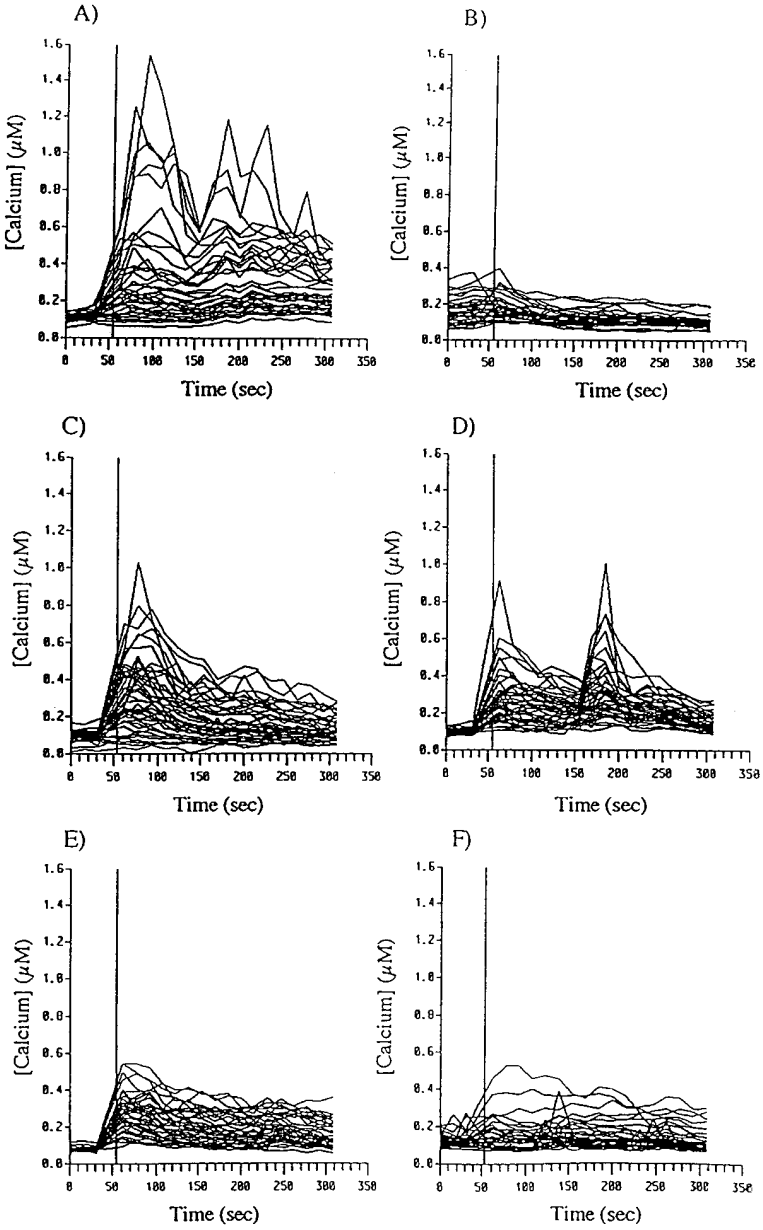


Figure 6. XeC and XeA Effectively Block $IP_3$-Mediated $Ca^{2+}$ Release and Oscillations in Primary Astrocytes

Each line indicates the $Ca^{2+}$ concentration over time in a single cell. Cells were loaded with indo-1 AM for 30 min prior to experimentation, and fluorescence was monitored using a scanning confocal fluorescent microscope, as described in Experimental Procedures. Carbachol (1 mM) was added 55 s (indicator line) after a 30 min incubation with control buffer, XeC, or XeA.

(A) Paired control (XeC).

(B) XeC (20 μM).

(C) Paired control (XeA).

(D) XeA, 1 μM.

(E) XeA, 10 μM.

(F) XeA, 20 μM.

from Exmouth Gulf, Western Australia, in 1993. Whole animals were immediately frozen and stored at −20°C for 2 years. The sponge was identified by Mary Kay Harper, Scripps Institution of Oceanography (La Jolla, CA). XeA, XeC, and ArB were isolated from Sample A (collected at a depth of −2 m), and XeD and DMXeB were isolated from sample B (collected at −10 m).

**Isolation and Characterization of Xe's**

Each sponge sample was processed in a similar manner, and purification of active fractions was assessed for their ability to inhibit $IP_3$-induced $Ca^{2+}$ release from vesicles as described below. Lyophilized sponge tissue was exhaustively extracted with methanol at 25°C (three times), and the combined methanol extract was concentrated to ~500 ml. The methanol extract was adjusted to ~10% v/v $H_2O$ and extracted with *n*-hexane. The aqueous methanol layer was adjusted to 20% $H_2O$ and extracted with chloroform. Finally, the methanol was removed from the aqueous fraction under reduced pressure, and the residue was extracted with *n*-butanol. $IP_3R$ inhibitory activity was located in the chloroform soluble fraction, which was further purified by column chromatography over silica gel (230–400 mesh, elution with a stepped gradient of 100:0 chloroform–methanol to 0:100 chloroform–methanol). Final purification of the active fractions was achieved by high-pressure liquid chromatography using two different conditions and detection by differential refractometry. The active fraction from sample A was separated on a normal phase silica high-pressure liquid chromotography column (Rainin Dynamax Si, 25 × 300 mm, 1:4 hexane: 2-propanol, containing 0.5% triethylamine, 3 ml/min) to give XeA (0.02% of dry weight) (Nakagawa et al., 1984), XeC (0.03% of dry weight) (Nakagawa et al., 1984), and ArB (0.017% of dry weight) (Kitagawa et al., 1989; Hoye et al., 1994, 1995). The active fraction from B was purified on an amino-bonded column (Rainin Dynamax $NH_2$, 25 × 300 mm, 98:2 hexane: 2-propanol containing 0.05% triethylamine, 3 ml/min) to provide pure XeD (0.0089% of dry weight) (Nakagawa et al., 1984) and DMXeB (0.0084% of dry weight) (Quirion et al., 1992). The structures were identified by comparison of $^1H$ and $^{13}C$ NMR data of purified compounds with those of literature values (Nakagawa et al., 1984; Kitagawa et al., 1989; Quirion et al., 1992; Hoye et al., 1994, 1995).

In order to examine how the three-dimensional molecular structure of Xe/araguspongine alkaloids might relate to their ability to

block the $IP_3$-activated pore, solution structures of XeA, XeC, and ArB were calculated using force field molecular mechanics (MM2) (Chem3D Plus, Cambridge Scientific Computing, Cambridge, MA). The atomic coordinates X-ray crystal structure of XeC (Cambridge Crystallographic Data Center, Cambridge, England) were used as the starting point for MM2 minimization to obtain quantitative structural information for XeC. The MM2 structure of XeA was obtained by force field minimization of a hybrid set of atomic coordinates for XeA. The hybrid data set, in turn, was generated by bond bisection of the dimeric XeC crystal structure, discarding the *cis*-ring heterobicycle and religating two copies of the *trans*-monomer. Both structures preserve the chair–chair conformations of the oxaquinolizidine ring. Distance-dependent dielectric factors were not used in the calculations, and the minimized structures do not take into account possible water of solvation.

**Membrane Preparations**

Microsomes enriched with the $IP_3R$ were isolated from the cerebellum of 2.5–3 kg male New Zealand white rabbits. Tissue was homogenized with a Potter-Elvehjem homogenizer in 10× (w/v) ice-cold buffer containing 5 mM HEPES (pH 7.4), 320 mM sucrose, 250 μM phenylmethylsulfonyl fluoride, and 5 μg/ml leupeptin. Microsomes were subsequently isolated by differential centrifugation (8,000–100,000 × g pellet). The final microsomal pellet was resuspended with a Dounce homogenizer in buffer lacking protease inhibitors at a protein concentration of 5–10 mg/ml. Microsomes were aliquoted into vials, quickly frozen in liquid nitrogen, and stored at −80°C.

Membrane vesicles enriched in $Ry_1R$ were isolated from the fast-twitch (white) skeletal muscle of the hind limbs and back of 3–4 kg male New Zealand white rabbits. Freshly ground muscle was homogenized in a Waring blender with 4 v of ice-cold homogenization buffer composed of 5 mM imidazole–HCl (pH 7.4), 0.3 M sucrose, 10 μg/ml leupeptin, and 100 μM phenylmethylsulfonyl fluoride. The junctional SR fraction was purified from a discontinuous sucrose gradient as previously described by Saito et al. (1984). The junctional SR fraction was collected from the 38%–45% sucrose interface, pelleted, and then resuspended in ice-cold homogenization buffer at a protein concentration of 3–5 mg/ml. Membranes were aliquoted into vials, quickly frozen in liquid nitrogen, and stored at −80°C. Protein concentrations were determined using the Lowry method (Lowry et al., 1951), with BSA as the standard.

**Cell Culture**

PC12 cells were obtained from American Type Culture Collection (Rockville, MD) and cultured at 37°C, 5% $CO_2$ in RPMI 1640 media supplemented with 2.05 mM L-glutamine, 10% heat-inactivated horse serum (at 56°C for 30 min), 5% fetal bovine serum, 100 U/ml penicillin, and 100 μg/ml streptomycin on 75 $cm^2$ Primaria tissue culture flasks (Falcon 3824, Becton Dickinson, Lincoln Park, NJ). Media was changed every 2 days, and cells were passaged biweekly. PC12 cells were plated on laminin-coated glass rectangular (9 × 22 cm) or round (d = 2.5 cm) coverslips at a density of $1 \times 10^5$ cells/$cm^2$. Cells were used for experiments 2–3 days after plating.

Primary rat cortical astrocyte cultures were prepared by a modification of the method of McCarthy and De Vellis (1980), as described previously (Guizzetti et al., 1996). Briefly, the cortices from day 21 fetuses (B&K Universal, Kent, WA) were minced, trypsinized, and washed three times by centrifugation with Dulbecco's Modified Eagle Medium supplemented with 10% fetal bovine serum. The tissue was triturated, filtered, and plated in 75 $cm^2$ flasks, previously coated with poly-*d*-lysine, at $1.5 \times 10^5$ cells/$cm^2$. Within 24 hr of plating, the flasks were shaken, and fresh media was added. Flasks were maintained at 37°C with 5% $CO_2$ for 9 days and fed every 3–4 days. On day 9 in culture, the flasks were shaken overnight, trypsinized, and reseeded in two-well cover glass chamber slides (Nunc 178656, Intermountain Scientific, Bountiful, UT), previously coated with poly-*d*-lysine, at $2.4 \times 10^5$ cells/$cm^2$. Following reseeding, astrocytes were grown for 2 days, then rinsed with phosphate-buffered saline, and serum-deprived for 2 days in Dulbecco's Modified Eagle Medium supplemented with 0.1% Fraction V fatty acid–free BSA. Astrocyte cultures were determined to be at least 95% pure by indirect immunofluorescence with antibodies against glial fibrillary acidic protein and neuron-specific enolase (Accurate Chemical, Westbury, NY).

**Calcium Transport Measurements**

Release of $Ca^{2+}$ from cerebellar and skeletal membrane vesicles was measured with the metallochromic dye antipyrylazo III in a diode array spectrophotometer (model 8542, Hewlett Packard, Palo Alto, CA).

Cerebellar microsomes were batch-loaded with $Ca^{2+}$ overnight (20 hr) at 4°C in $Ca^{2+}$ transport buffer (8 mM K-MOPS [pH 7.0], 40 mM KCl, 62.5 mM $KH_2PO_4$, and 250 μM antipyrylazo III) containing 80–160 μg/ml creatine phosphokinase, 20–40 mM phosphocreatine, 4–8 mM Mg–ATP, 4 mM $NaN_3$, 40 μg/ml leupeptin, 100 μM $CaCl_2$, and 333–667 μg/ml cerebellar microsomal protein. Calcium-loaded microsomes were then diluted 1:3 in $Ca^{2+}$ transport buffer lacking microsomes (final volume 1.2 ml). Upon warming the solution to 37°C (500 s), the ability of Xe's/araguspongines to block $IP_3$ (5 μM)-induced $Ca^{2+}$ release was assessed in temperature-controlled cuvettes with constant stirring.

Skeletal vesicles (50 μg protein/cuvette) were loaded with $Ca^{2+}$ in $Ca^{2+}$ transport buffer containing 18.5 mM K-MOPS (pH 7.0), 92.5 mM KCl, 7.5 mM sodium pyrophosphate, 250 μM antipyrylazo III, 1 mM Mg–ATP, 20 μg/ml creatine phosphokinase, and 5 mM phosphocreatine, with a final volume of 1.2 ml. Immediately prior to measuring caffeine-induced $Ca^{2+}$ release, vesicles were loaded to near capacity with serial additions of 24 nmol $CaCl_2$ in temperature-controlled cuvettes (37°C) with constant stirring. The ability of XeC (0.1–10 μM) to block caffeine (20 mM)-induced $Ca^{2+}$ release via $Ry_1R$ was determined after the dye signal returned to baseline following loading.

Calcium transport was measured using a multisample transporter to sequentially measure two samples. Changes in extravesicular free $Ca^{2+}$ were determined by subtracting the antipyrylazo III absorbance at 790 nm from the absorbance at 710 nm. For each curve, methanol controls were acquired simultaneously to normalize the degree of inhibition found in the samples containing Xe. In each experiment, absorbance signals were calibrated by the addition of 1.0 μg of the $Ca^{2+}$ ionophore, A23187, followed by 20 or 24 nmol additions of $CaCl_2$ from a National Bureau of Standards stock solution. Initial $Ca^{2+}$ release rates were determined by linear regression analysis of the first 15–50 s of $Ca^{2+}$ release.

**[$^3$H]$IP_3$ Binding Assay**

Specific binding of [$^3$H]$IP_3$ to cerebellar microsomes was determined according the methods of Mohr et al. (1993) with minor modifications. The ability of XeC to block the binding of 1 nM [$^3$H]$IP_3$ to high-affinity sites on cerebellar microsomes (200 μg protein) dose dependently was assayed in a buffer containing 100 mM KCl, 20 mM NaCl, 1 mM EDTA, 0.1% BSA, and 25 mM $Na_2HPO_4$ (pH 8.0). XeC (1–10 μM) was added to cerebellar microsomes, and the binding reaction was initiated with addition of [$^3$H]$IP_3$ assay buffer (1 ml final volume). Tubes were incubated at 4°C with constant shaking. After 30 min, assays were terminated by rapid, single manifold filtration through Whatman GF/B filters presoaked with ice-cold assay buffer, followed by immediate washing of filters with 2.5 ml ice-cold assay buffer. Filters were soaked overnight in 5 ml scintillation cocktail, and the radioactivity on the filters was measured using a liquid scintillation counter. Nonspecific binding was measured in the presence of a 500-fold excess of unlabeled $IP_3$.

**[$^3$H]Ryanodine Binding Assay**

Specific binding of [$^3$H]ryanodine to skeletal membrane vesicles was determined according to the methods of Pessah et al. (1987). The ability of XeC to dose dependently block the binding of 1 nM [$^3$H]ryanodine to high-affinity sites on skeletal SR (50 μg protein) was assayed in a buffer consisting of 20 mM HEPES (pH 7.1), 250 mM KCl, 15 mM NaCl, 10% sucrose, and 50 μM $CaCl_2$. XeC (0.1–10 μM) was added to skeletal microsomes, and the binding reaction was initiated with addition of [$^3$H]ryanodine assay buffer (500 μl final volume). Following incubation for 3 hr at 37°C, assays were terminated by rapid filtration, with a Brandel (Gaithersburg, MD) cell harvester, through Whatman GF/B glass fiber filters. Filters were rinsed three times with 2 ml ice-cold harvest buffer (20 mM Tris–HCl [pH

7.1], 250 mM KCl, 15 mM NaCl, and 50 μM $CaCl_2$) and soaked overnight in 5 ml scintillation cocktail. Radioactivity on the filters was measured with a liquid scintillation counter. Nonspecific binding of [$^3$H]ryanodine was determined by the addition of 1000-fold excess of cold ryanodine.

### Fluorometric Measurements of Cytosolic Calcium in Intact Cells

Two to three days following plating, intracellular $Ca^{2+}$ was measured from PC12 cell populations either using a fluorometer (model F-2000, Hitachi, Japan) or ratiofluorescence video imaging (Photon Technology International, Princeton, NJ). Cells were loaded with a 5 μg/ml solution of cell permeant fura-2 acetoxymethyl ester (fura-2 AM, Molecular Probes, Eugene, OR) in imaging buffer (125 mM NaCl, 5 mM KCl, 2 mM $KH_2PO_4$, 1.2 mM $MgSO_4$, 2 mM $CaCl_2$, 25 mM HEPES, 6 mM glucose, 0.05% BSA [fraction 5], and 250 μM sulfinpyrazone [pH 7.4]) for 30 min at 25°C. PC12 cells were then rinsed twice and stored in imaging buffer until needed (0 or 30 min). Coverslips were left to equilibrate for 2–3 min in imaging buffer before measurements began. In initial experiments, MeOH (10 μl) or Xe's (20 μM) were added 2 min after recording began, and bradykinin (300 nM) or ionomycin (5 μM) was added 10 min later. Measurements performed in $Ca^{2+}$-depleted media were made by addition of EGTA (3 and 5 mM final concentrations) 1 min prior to bradykinin/ionomycin addition, to obtain free $Ca^{2+}$ levels of 120 and 40 nM, respectively. In the experiments examining the XeC dose–response relationship and effect of Xe's on the RyR, PC12 cells were incubated with MeOH (4 or 10 μl) or XeC (5–20 μM) for 30 min and 20 min, respectively, in buffer lacking 0.05% BSA, before bradykinin addition. Measurements were performed at a constant 37°C in continually stirred cuvettes (photometry) or a clamp chamber (imaging). The arbitrary fluorescence units of 340 nm/380 nm were used to compare the Xe-treated and control cell populations.

Calcium measurements on primary rat cortical astrocyte cultures were carried out by a modification of the method of Kovacs et al. (1995). At the time of the experiment, media was removed, and cells were rinsed twice with Krebs bicarbonate buffer and loaded with a 2 μM solution of cell permeant indo-1 acetoxymethyl ester (indo-1 AM, Molecular Probes, Eugene, OR) in Krebs buffer, containing 1% Fraction V BSA, 0.001% lipids-cholesterol-rich solution, and 1 mM probenecid, for 30 min at 37°C. Following loading, cells were rinsed with Krebs buffer, without BSA and lipids, and incubated for at least 15 min at 37°C to allow for cleavage of the indo-1 AM ester. Indo-1 was excited at 351–363 nm, and emission was detected simultaneously at 405 and 530 nm to measure the fluorescence intensity of the dye bound and not bound to $Ca^{2+}$, respectively. Fluorescence measurements were made using an attached-cell analysis and sorter Ultima instrument (Meridian Instruments, Okemos, MI). The ratio of the fluorescence at the two wavelengths was determined and was compared to the ratio for $Ca^{2+}$ standard in solution (Molecular Probes, Eugene, OR) to determine the absolute $Ca^{2+}$ concentration. The fluorescence within 50 cells was quantified over time for each treatment. For Xe experiments, cells were preincubated with the inhibitor for 30 min. Prior to carbachol addition, baseline $Ca^{2+}$ measurements were determined by three scans conducted at 15 s intervals. After the third scan, a 30 s lapse in scanning allowed for the addition of carbachol (1 mM), and then $Ca^{2+}$ changes were monitored every 15 s for 17 scans.

### Measurements of Acute Cytotoxicity

In order to assess the acute toxicity of Xe's, trypan blue staining and LDH measurements were performed on PC12 cells and primary astrocyte cultures, respectively. Two days after plating, 4 μl MeOH or 20 μM XeC was added to PC12 cells, and cells were left to incubate at 37°C, 5% $CO_2$ for 10 or 30 min. Following incubation, media was removed, 0.4% trypan blue in culture media (1:3 v/v) was added, and 10 fields of view (100×) were assessed for the presence of dead cells. Triton X-100 (0.1%)-treated cells were used as a positive control. In astrocyte cultures, the levels of LDH in the media were measured following treatment of cells with 20 μM XeC for 30 min. Incubation for 30 min with buffer alone or a cytotoxic concentration of Triton X-100 (0.1%) were used as controls. LDH levels were measured using the Sigma Diagnostics LDH optimized lactate-dehydrogenase EC 1.1.1.27 UV-test kit (catalog No. DG1340-K).

### Acknowledgments

The authors would like to thank Helen Kim for her assistance in the transport assays and Tom Chavez for his contribution to the ryanodine binding studies. We thank Marilyn Olmstead for assistance with conversion of the fraction crystal coordinates of XeC. This work was supported by National Institutes of Health Training Grant ES07059 (J. G.), RO1 ES05002 (I. N. P.), RO1 AI39987 and RO1 AI31660 (T. F. M.), RO1 AA08154 and P30 ES07033 (L. G. C.), and by a Grant-in-Aid of Research from the National Academy of Sciences through Sigma Xi, The Scientific Research Society (J. A. M.).

Received April 4, 1997; revised July 14, 1997.

### References

Arrang, J.M. (1994). Pharmacological properties of histamine receptor subtypes. Cell. Mol. Biol. *40*, 275–281.

Berridge, M.J. (1993). Inositol trisphosphate and calcium signaling. Nature *361*, 315–325.

Bezprozvanny, I.B., Ondrias K., Kaftan E., Stoyanovsky D.A., and Ehrlich, B.E. (1993). Activation of the calcium release channel (ryanodine receptor) by heparin and other polyanions is calcium dependent. Mol. Biol. Cell *4*, 347–352.

Brann, M.R., Klimkowski, V.J., and Ellis, J. (1993). Structure/function relationships of muscarinic acetylcholine receptors. Life Sci. *52*, 405–412.

Bretschneider, E., Paintz, M., and Glusa, E. (1995a). Inositol 1, 4, 5-trisphosphate and protein kinase C are involved in thrombin- and trap-induced vascular smooth muscle contraction. Agents Actions Suppl. *45*, 309–313.

Bretschneider, E., Paintz, M., and Glusa, E. (1995b). Involvement of inositol 1, 4, 5-trisphosphate and protein kinase C in thrombin-induced contraction of porcine ulmonary artery. Biochem. Pharmacol. *49*, 33–38.

Briner, V.A., Tsai, P., and Schrier, R.W. (1993). Bradykinin: potential for vascular constriction in the presence of endothelial injury. Am. J. Physiol. *264*, F322–F327.

Cameron, A.M., Steiner, J.P., Sabatini, D.M., Kaplin, A.I., Walensky, L.D., and Snyder, S.H. (1995). Immunophilin FK506-binding protein associated with inositol 1,4,5-trisphosphate receptor modulates calcium flux. Proc. Natl. Acad. Sci. USA *92*, 1784–1788.

Crews, P., Slate, D.L., Gerwick, W.H., Schmitz, F.J., Scatzman, R., Strulovici, B., Cannon, P., and Hunter, L.M. (1994). Screening for anticancer leads from marine organisms in a mechanism-based drug delivery program. Dev. Oncol. *74*, 364–403.

Dauphin, F., Linville, D.G., and Hamel, E. (1994). Cholinergic dilatation and constriction of feline cerebral blood vessels are mediated by stimulation of phosphoinositide metabolism via two different muscarinic receptor subtypes. J. Neurochem. *63*, 544–551.

Endo, M., Nakagawa, M., Hamamoto, Y., and Ishihama, M. (1986). Pharmacologically active substances from southern Pacific marine invertebrates. Pure Appl. Chem. *58*, 387–394.

Fasolato, C., Zottini, M., Clementi, E., Zacchetti, D., Meldolesi, J., and Pozzan, T. (1991). Intracellular $Ca^{2+}$ pools in PC12 cells. J. Biol. Chem. *266*, 20159–20167.

Furuichi, T., Yoshikawa, S., Miyawaki, A., Wada, K., Maeda, N., and Mikoshiba, K. (1989). Primary structure and functional expression of the inositol 1,4,5-trisphosphate-binding protein P400. Nature *342*, 32–38.

Ghosh, T.K., Eis, P.S., Mullaney, J.M., Ebert, C.L., and Gill, D.L. (1988). Competitive, reversible, and potent antagonism of inositol 1,4,5-trisphosphate-activated calcium release by heparin. J. Biol. Chem. *263*, 11075–11079.

Grohovaz, F., Zacchetti, D., D'Andrea, P., Lorenzon, P., and Meldolesi, J. (1992). $[Ca^{2+}]_i$ effects of bradykinin B2 receptor activation in PC12 cells. Agents Actions. Suppl. *38*, 9–15.

Guizzetti, M., Costa, M., Peters, J., and Costa, L.G. (1996). Acetylcholine as a mitogen: muscarinic receptor-mediated proliferation of rat astrocytes and human astrocytoma cells. Eur. J. Pharmacol. *297*, 265–273.

Harnick, D.J., Jayaraman, T., Ma, Y., Mulieri, P., Go, L.O., and Marks, A.R. (1995). The human type 1 inositol 1,4,5-trisphosphate receptor from T lymphocytes. Structure, localization, and tyrosine phosphorylation. J. Biol. Chem. *270*, 2833–2840.

Hoye, T.R., North, J.T., and Yao, L.J. (1994). Conformational considerations in 1-oxaquinolizidines related to the xestospongin/araguspongine family: reassignment of stereostructures for araguspongines B and E. J. Org. Chem. *59*, 6904–6910.

Hoye, T.R., North, J.T., and Yao, L.J. (1995). Conformational considerations in 1-oxaquinolizidines related to the xestospongin/araguspongine family: reassignment of stereostructures for araguspongines B and E. J. Org. Chem. *60*, 4958.

Kitagawa, I., Kobayashi, M., and Kawazoe, K. (1989). Araguspongines B, C, D, E, F, G, H, and J, new vasodilative bis-1-oxaquinolizidine alkaloids from an okinawan marine sponge, *Xestospongia sp*. Chem. Pharm. Bull. (Tokyo) *37*, 1676–1678.

Kobayashi, S., Somlyo, A.V., and Somlyo, A.P. (1988). Heparin inhibits the inositol 1,4,5-trisphosphate-dependent, but not the independent, calcium release induced by guanine nucleotide in vascular smooth muscle. Biochem. Biophys. Res. Commun. *153*, 625–631.

Kovacs, K.A., Kavanagh, T.J., and Costa, L.G. (1995). Ethanol inhibits muscarinic receptor-stimulated phosphoinositide metabolism and calcium mobilization in rat primary cortical cultures. Neurochem. Res. *20*, 939–949.

Lowry, O.H., Rosebrough, N.J., Farr, A.L., and Randall, R.J. (1951). Protein measurement with folin phenol reagent. J. Biol. Chem. *193*, 265–275.

Maranto, A.R. (1994). Primary structure, ligand binding, and localization of the human type 3 inositol 1,4,5-trisphosphate receptor expressed in intestinal epithelium. J. Biol. Chem. *269*, 1222–1230.

Marks, A.R. (1996). Cellular functions of immunophilins. Physiol. Rev. *76*, 631–649.

McCarthy, K.D., and De Vellis, J. (1980). Preparation of separate astroglial and oligodendroglial cell cultures from rat cerebral tissue. J. Biol. Chem. *85*, 890–902.

Mignery, G.A., Südhof, T.C., Takei, K., and De Camilli, P. (1989). Putative receptor for inositol 1,4,5-trisphosphate similar to ryanodine receptor. Nature *342*, 192–195.

Mignery, G.A., Newton, C.L., Archer, B.T.d., and Südhof, T.C. (1990). Structure and expression of the rat inositol 1,4,5-trisphosphate receptor. J. Biol. Chem. *265*, 12679–12685.

Mohr, F.C., Hershey, P.E., Zimanyi, I., and Pessah, I.N. (1993). Regulation of inositol 1,4,5-trisphosphate receptors in rat basophilic leukemia cells. I. Multiple conformational states of the receptor in a microsomal preparation. Biochem. Biophys. Acta *1147*, 105–114.

Nakade, S., Maeda, N., and Mikoshiba, K. (1991). Involvement of the C-terminus of the inositol 1,4,5-trisphosphate receptor in $Ca^{2+}$ release analysed using region-specific monoclonal antibodies. Biochem. J. *277*, 125–131.

Nakagawa, M., Endo, M., Tanaka, N., and Gen-Pei, L. (1984). Structures of xestospongin A, B, C and D, novel vasodilative compounds from marine sponge, *Xestospongia exigua*. Tetrahedron Lett. *25*, 3227–3230.

Nakanishi, S., Maeda, N., and Mikoshiba, K. (1991). Immunohistochemical localization of an inositol *1*,4,5-trisphosphate receptor, P400, in neural tissue: studies in developing and adult mouse brain. J. Neurosci. *11*, 2075–2086.

Pessah, I.N., Stambuk, R.A., and Casida, J.E. (1987). $Ca^{2+}$-activated ryanodine binding: mechanisms of sensitivity and intensity modulation by $Mg^{2+}$, caffeine, and adenine nucleotides. Mol. Pharmacol. *31*, 232–238.

Pessah, I.N., Molinski, T.F., Meloy, T.D., Wong, P., Buck, E.D., Allen, P.D., Mohr, F.C., and Mack, M.M. (1997). Bastadins relate ryanodine-sensitive and -insensitive $Ca^{2+}$ efflux pathways in skeletal SR and $BC_3H1$ cells. Am. J. Physiol. *272*, C601–C614.

Pettit, G.R., Orr, B., Herald, D.L., Doubek, D.L., Tackett, L., Schmidt, J.M., Boyd, M.R., Pettit, R.K., and Hooper, J.N.A. (1996). Isolation and x-ray crystal structure of racemic xestospongin D from the Singapore marine sponge *Niphates sp*. Bioorg. Med. Chem. Lett. *6*, 1313–1318.

Pin, J.-P., and Duvoisin, R. (1995). Review: neurotransmitter receptors I–the metabotropic glutamate receptors: structure and functions. Neuropharmacology *34*, 1–26.

Quirion, J.C., Sevenet, T., Husson, H.P., Weniger, B., and Debitus, C. (1992). Two new alkaloids from *Xestospongia sp*., a new Caledonian sponge. J. Nat. Prod. *55*, 1505–1508.

Ross, C.A., Danoff, S.K., Schell, M.J., Snyder, S.H., and Ullrich, A. (1992). Three additional inositol 1,4,5-trisphosphate receptors: molecular cloning and differential localization in brain and peripheral tissues. Proc. Natl. Acad. Sci. USA *89*, 4265–4269.

Saito, A., Seiler, S., Chu, A., and Fleischer, S. (1984). Preparation and morphology of sarcoplasmic reticulum terminal cisternae from rabbit skeletal muscle. J. Cell Biol. *99*, 875–885.

Südhof, T.C., Newton, C.L., Archer, B.T.d., Ushkaryov, Y.A., and Mignery, G.A. (1991). Structure of a novel $InsP_3$ receptor. EMBO J. *10*, 3199–3206.

Sullivan, K.M., Lin, D.D., Agnew, W., and Wilson, K.L. (1995). Inhibition of nuclear vesicle fusion by antibodies that block activation of inositol 1,4,5-trisphosphate receptors. Proc. Natl. Acad. Sci. USA *92*, 8611–8615.

Takeshima, H., Nishimura, S., Matsumoto, T., Ishida, H., Kangawa, K., Minamino, N., Matsuo, H., Ueda, M., Hanaoka, M., Hirose, T., et al. (1989). Primary structure and expression from complementary DNA of skeletal muscle ryanodine receptor. Nature *339*, 439–445.

Tinker, A., and Williams, A.J. (1995). Measuring the length of the pore of the sheep cardiac reticulum calcium-release channel using related molecular calipers. Biophys. J. *68*, 111–120.

Verma, A., Ross, C.A., Verma, D., Supattapone, S., and Snyder, S.H. (1990). Rat brain endoplasmic reticulum calcium pools are functionally segregated. Cell Regul. *1*, 781–790.

Yamada, N., Makino, Y., Clark, R.A., Pearson, D.W., Mattei, M.G., Guenet, J.L., Ohama, E., Fujino, I., Miyawaki, A., Furuichi, T., et al. (1994). Human inositol 1,4,5-trisphosphate type-1 receptor, $insP_3R1$: structure, function, regulation of expression and chromosomal localization. Biochem. J. *302*, 781–790.

Zacchetti, D., Clementi, E., Fasolato, C., Lorenzon, P., Zottini, M., Grohovoz, F., Fumagalli, G., Pozzan, T., and Meldolesi, J. (1991). Intracellular $Ca^{2+}$ pools in PC12 cells. J. Biol. Chem. *266*, 20152–20158.